WU B 09-06
August, 30 2009

An attempt to understand exclusive π^+ electroproduction

S.V. Goloskokov [1]

Bogoliubov Laboratory of Theoretical Physics, Joint Institute for Nuclear Research,
Dubna 141980, Moscow region, Russia

P. Kroll [2]

Fachbereich Physik, Universität Wuppertal, D-42097 Wuppertal, Germany
and
Institut für Theoretische Physik, Universität Regensburg,
D-93040 Regensburg, Germany
(revised version)

Abstract

Hard exclusive π^+ electroproduction is investigated within the handbag approach. The prominent role of the pion-pole contribution is demonstrated. It is also shown that the experimental data require a twist-3 effect which ensues from the helicity-flip generalized parton distribution H_T and the twist-3 pion wave function. The results calculated from this handbag approach are compared in detail with the experimental data on cross sections and spin asymmetries measured with a polarized target. It is also commented on consequences of this approach for exclusive π^0 and vector-meson electroproduction.

[1]Email: goloskkv@theor.jinr.ru
[2]Email: kroll@physik.uni-wuppertal.de

1 Introduction

With the advent of new, rather precise data on hard exclusive processes in recent years the interest in the theoretical analysis of such processes within QCD has strongly grown. The basis of such analyses is the factorization of the process amplitudes into hard subprocesses and soft hadronic matrix elements parameterized in terms of generalized parton distributions (GPDs). An indispensable purpose of such analyses is the scrutiny of this so-called handbag approach within the experimentally accessible kinematical region. It is to be examined for instance whether factorization holds or whether there is need for higher-twist and/or power corrections. Another task is to extract as much as possible qualitative and quantitative information about the GPDs. These functions embody the internal partonic structure of the hadrons. In addition to the longitudinal momentum distribution of the partons which is already provided by the usual parton distributions, the GPDs also incorporate the transverse distributions of the partons inside the proton. A fully model independent extraction of the GPDs from experiment is presumably impossible. Therefore one is likely dependent on models or parameterizations of the GPDs constraint by theoretical concepts. Frequently used is an integral representation of the GPDs where the integrand represents a the double distribution [1, 2]. This way the skewness dependence of the GPDs is generated. Other concepts have been exploited in recent analyses of deeply virtual Compton scattering: In [3] the GPDs are constraint by analyticity and in [4] a dual parameterization is employed.

In our recent analyses of vector-meson electroproduction [5, 6, 7] the double distribution method has been used. The rather small ratio of the longitudinal over transversal cross sections indicates the important role of transversely polarized virtual photons in the experimentally accessible range of photon virtualities. The transversely polarized photons manifestly lead to higher-twist and/or power corrections which are asymptotically suppressed by the inverse of the photon virtuality, $1/Q$, in the amplitudes. Here in this work we attempt an analysis of hard exclusive electroproduction of charged pions. The description of this process within the handbag approach presents a major challenge. Besides the differential cross sections measured by the $F_\pi - 2$ collaboration [8] and HERMES [9] which exhibit a pronounced forward spike, there are also data on spin asymmetries measured with a polarized target [10, 11]. Spin dependent observables typically probe subtle details of the amplitudes as for instance relative phases. The pertinent GPDs occur-

ring in π^+ electroproduction are the poorly known $\widetilde{H}$ and $\widetilde{E}$. This is to be contrasted with vector-meson electroproduction where mainly the GPDs H and E are probed. Electroproduction of pions has been investigated several times [12, 13, 14, 15] to leading-twist accuracy. It turns out that this naive although theoretically clean approach, fails by order of magnitude with the experimental cross section. The main reason for this disaster is the use of only the perturbative contribution to the pion form factor which is mandatory to leading-twist accuracy.

In the present analysis of π^+ electroproduction we are going to vary from the leading-twist approximation in several aspects. First we will make use of the modified perturbative approach [16] for the calculation of the subprocess amplitudes as we did for vector-meson electroproduction. Secondly we will use the full electromagnetic form factor of the pion instead of only its much smaller perturbative contribution. Thirdly, we will allow for contributions from the GPD $\widetilde{E}$ and lastly, we will take into account a twist-3 effect which involves the helicity-flip GPD H_T [17]. As we are going to demonstrate below the data on the spin asymmetry obtained with a transversely polarized target [10] demand this contribution. With respect to the fact that we need three (almost) unknown GPDs for exclusive π^+ electroproduction we consider our analysis as a rather qualitative study, not all aspects of the data will be accommodated well. Yet we think of our work as the next step towards a comprehensive analysis of hard exclusive meson electroproduction.

The plan of the paper is the following: In the next section we will briefly sketch the description of the leading longitudinal amplitude within the hand-bag approach. In Sect. 3 we will present the pion-pole contribution. In Sect. 4 we will demonstrate the need for contributions from transversely polarized virtual photons in π^+ production and thereafter describe the twist-3 mechanism (Sect. 5). In Sect. 6 we will present the model GPDs and the pion wave functions. Our results are compared to experiment in Sect. 7. Sects. 8 and 9 are devoted to a brief discussion of implications of our approach for exclusive π^0 and vector-meson electroproduction, respectively. A remarks on a symmetry property of the helicity amplitudes are presented in Sect. 10. We close the paper with a summary (Sect. 11). In an Appendix we compile the relations between various observables of π electoproduction and helicity amplitudes.

2 The leading amplitudes

In the GPD-based handbag factorization scheme it can be shown [18] that for large photon virtualities but small invariant momentum transfer, t, from the incoming to the outgoing baryon, the amplitudes for longitudinally polarized photons $\mathcal{M}_{0\nu',0\nu}$ dominate the process $\gamma^* p \to \pi^+ n$. Here, ν and ν' label the helicities of the proton and neutron, respectively. The amplitudes for transversely polarized photons are suppressed by $1/Q$ against the longitudinal ones.

Within the handbag approach the amplitudes for pion electroproduction through longitudinally polarized photons read

$$\begin{aligned}
\mathcal{M}^{\pi^+}_{0+,0+} &= \sqrt{1-\xi^2}\,\frac{e_0}{Q}\Big[\langle\widetilde{H}^{(3)}\rangle - \frac{\xi^2}{1-\xi^2}\langle\widetilde{E}^{(3)}\rangle - \frac{2\xi m Q^2}{1-\xi^2}\frac{\rho_\pi}{t-m_\pi^2}\Big]\,, \\
\mathcal{M}^{\pi^+}_{0-,0+} &= \frac{e_0}{Q}\,\frac{\sqrt{-t'}}{2m}\Big[\xi\langle\widetilde{E}^{(3)}\rangle + 2mQ^2\frac{\rho_\pi}{t-m_\pi^2}\Big]\,. \qquad (1)
\end{aligned}$$

Here, the usual abbreviation $t' = t - t_0$ is employed where $t_0 = -4m^2\xi^2/(1-\xi^2)$ is the minimal value of t corresponding to forward scattering. The mass of the nucleon is denoted by m and the skewness parameter, ξ, is related to Bjorken-x by

$$\xi \;=\; \frac{x_{\rm Bj}}{2 - x_{\rm Bj}}\,. \qquad (2)$$

Helicity flips at the baryon vertex are taken into account since they are only suppressed by $\sqrt{-t'}/m$. In contrast to this, effects of order $\sqrt{-t'}/Q$ are neglected.

The pion pole contribution, see Fig. 1, with the residue ρ_π and pion mass m_π, will be discussed in the next section in some detail. In constrast to other work [12, 13, 14, 15] but in view of the fact that we take into account the full pion form factor and not just its perturbative contribution, we write the pion pole contributions and those from $\widetilde{E}^{(3)}$ separately, i.e. our $\widetilde{E}^{(3)}$ only represents the non-pole contribution of the full GPD. For large Q^2, $\rho_\pi \propto 1/Q^2$ so that all terms in (1) possess the same scaling behavior. The item $\langle\widetilde{F}\rangle$ denotes a convolution of a GPD $\widetilde{F}(=\widetilde{H},\widetilde{E})$ and an appropriate subprocess amplitude to be calculated from Feynman graphs of which a typical lowest order example is shown in Fig. 1,

$$\langle\widetilde{F}^{(3)}\rangle \;=\; \sum_\lambda \int_{-1}^{1} d\bar{x}\,\mathcal{H}_{0\lambda,0\lambda}(\bar{x},\xi,Q^2,t=0)\,\widetilde{F}^{(3)}(\bar{x},\xi,t)\,. \qquad (3)$$

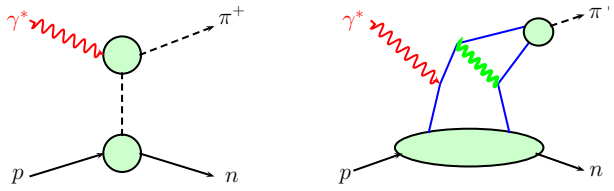

Figure 1: The pion pole (left) and the handbag (right) contribution to electroproduction of positively charged pions.

The label λ refers to the unobserved helicities of the partons participating in the subprocess. For π^+ production the $p \to n$ transition GPDs are required which are given by the isovector combination of proton GPDs [13, 14]

$$\widetilde{F}^{(3)} \;=\; \widetilde{F}^u - \widetilde{F}^d \,. \tag{4}$$

If the sea-quark GPDs are flavor symmetric only the differences of the valence quark GPDs contribute to π^+ electroproduction.

As in our previous work on hard electroproduction of vector mesons [5, 6, 7] we calculate the $\gamma^* q \to \pi q$ subprocess amplitudes within the modified perturbative approach [16] in which quark transverse degrees of freedom as well as Sudakov suppressions are taken into account. Since the re-summation of the logarithms involved in the Sudakov factor can only be performed in the impact parameter space efficiently [16] we quote the subprocess amplitudes in that space

$$\begin{aligned} \mathcal{H}_{0\lambda,0\lambda} \;&=\; \int d\tau d^2b\, \hat{\Psi}_\pi(\tau,-\mathbf{b})\, \hat{\mathcal{F}}^{(3)}_{0\lambda,0\lambda}(\bar{x},\xi,\tau,Q^2,\mathbf{b}) \\ &\quad \times \alpha_{\rm s}(\mu_R)\exp[-S(\tau,\mathbf{b},Q^2)]\,. \end{aligned} \tag{5}$$

For the Sudakov factor S, the choice of the renormalization (μ_R) and factorization scales as well as the hard scattering kernels $\mathcal{F}$ or their respective Fourier transforms $\hat{\mathcal{F}}$, we refer to Ref. [7]. The last item in (5) to be explained is $\hat{\Psi}_\pi(\tau,-\mathbf{b})$ which represents the Fourier transform of the momentum-space light-cone wave function (LCWF) for the pion (τ is the momentum fraction of the quark that enters the meson, defined with respect to the meson momentum). It is to be emphasized that parton transverse momenta are only taken into account in the subprocess while the partons entering the subprocess are viewed as being emitted and re-absorbed by the nucleon collinearly.

This approximation is justified to some extent by the fact that the GPDs describe the full proton whereas the meson is only generated through its compact valence Fock state. For a detailed discussion of the modified perturbative approach and its application to hard meson electroproduction we refer to [5, 6, 7].

For the ease of comparison with other work we quote the momentum-space subprocess amplitude in collinear approximation where the pion wave function reduces to its associated leading-twist distribution amplitude:

$$\sum_{\lambda} \mathcal{H}_{0\lambda,0\lambda} \;=\; \frac{C_F}{N_c} 4\pi\alpha_{\rm s}(\mu_R) f_\pi \langle 1/\tau \rangle_\pi \Big[\frac{e_u}{\bar{x}-\xi+\imath\varepsilon} + \frac{e_d}{\bar{x}+\xi-\imath\varepsilon} \Big] , \qquad (6)$$

where $f_\pi (= 131\ \text{MeV})$ denotes the pion decay constant and $\langle 1/\tau \rangle_\pi$ the $1/\tau$ moment of the pion's distribution amplitude. The color factor C_F is given by $(N_c^2-1)/(2N_c)$ where N_c the number of colors. Finally, e_a is the charge of quarks of flavor a in units of the positron charge e_0. The running coupling $\alpha_{\rm s}$ is evaluated from the one-loop expression with $\Lambda_{\rm QCD} = 240\ \text{MeV}$.

3 The pion-pole contribution

The pion exchange graph shown in Fig. 1, leads to the following contribution to the helicity amplitudes of the process $\gamma^* p \to \pi^+ n$

$$\mathcal{M}^{\rm pole}_{0\nu',\mu\nu} \;=\; e_0 \frac{\rho_\pi}{t-m_\pi^2} \, (2q'-q)\cdot\epsilon(\mu)\, \bar{u}(p',\nu')\gamma_5 u(p,\nu) \, , \qquad (7)$$

where p, p', q' and q are the momenta of the proton, neutron, pion and photon, respectively. The polarization vector of the virtual photon is denoted by ϵ and its helicity by μ. The residue of the pole is given by

$$\rho_\pi \;=\; \sqrt{2} g_{\pi NN} F_\pi(Q^2) F_{\pi NN}(t') \, . \qquad (8)$$

The coupling of the pion to the nucleon is given by the familiar pion-nucleon coupling constant, $g_{\pi NN}$, for which we take the value 13.4. The structure of the pion and the nucleon is taken into account by form factors, the electromagnetic one for the pion, $F_\pi(Q^2)$, whereby the small virtuality of the exchanged pion is as usual ignored, and $F_{\pi NN}(t)$ for the π-nucleon vertex.

Working out the spinor expression (7), one obtains for the helicity amplitudes at small $-t$ and large Q^2

$$
\begin{aligned}
\mathcal{M}^{\rm pole}_{0+,0+} &= -e_0 \frac{2m\xi Q}{\sqrt{1-\xi^2}} \frac{\rho_\pi}{t-m_\pi^2}\,, \\
\mathcal{M}^{\rm pole}_{0-,0+} &= +e_0 Q\sqrt{-t'}\,\frac{\rho_\pi}{t-m_\pi^2}\,, \\
\mathcal{M}^{\rm pole}_{0+,\pm+} &= \pm 2\sqrt{2} e_0 \xi m \sqrt{-t'}\,\frac{\rho_\pi}{t-m_\pi^2}\,, \\
\mathcal{M}^{\rm pole}_{0-,\pm+} &= \pm\sqrt{2} e_0 t' \sqrt{1-\xi^2}\,\frac{\rho_\pi}{t-m_\pi^2}\,. \qquad (9)
\end{aligned}
$$

Terms suppressed by $1/Q^2$ against the longitudinal amplitudes, in particular terms of order t'/Q^2, are neglected in order to be compatible with the approximations used for the GPD contributions.

As one may see from the relations (9) the pion-pole contributions to the amplitudes for transversely polarized photons vanish for forward scattering. One would therefore expect a forward dip in the cross section for photoproduction of pions or other pion-exchange dominated reactions like $p\bar{p} \to n\bar{n}$ or proton-neutron charge exchange. However, this expectation is in sharp contrast to the behavior of the experimental cross sections which rather exhibit pronounced forward spikes with widths of order of the pion mass squared. Hence, one is compelled to conclude that there is another contribution that conspires with the pion contribution in such a way that a non-vanishing forward cross section is generated [20]. A popular dynamical realization of such a conspirator is the so-called poor man's absorption model [21] in which the $L = 0$ partial wave of this amplitude is absorbed completely. Effectively this prescription consists of replacing the factor t' in the helicity non-flip amplitude $\mathcal{M}^{\rm pole}_{0-,++}$ by m_π^2. It is important to realize in this context that this amplitude has no net helicity flip. The factor t' occurring in it (cf. (9)) is a dynamical effect and not forced by angular momentum conservation [3]. The mentioned replacement can be viewed as the net effect of adding a smooth background to the pole term [22]

$$
\begin{aligned}
\mathcal{M}^{\rm pole}_{0-,++} &\implies \mathcal{M}^{\rm pole}_{0-,++} + \sqrt{2} e_0 \rho_\pi \sqrt{\frac{1+\xi}{1-\xi}} \\
&\simeq \sqrt{2} e_0 (t_0 - m_\pi^2) \sqrt{\frac{1+\xi}{1-\xi}} \frac{\rho_\pi}{t-m_\pi^2}\,. \qquad (10)
\end{aligned}
$$

[3] For $t' \to 0$ a helicity amplitude vanishes (at least) as $\mathcal{M}_{\mu'\nu',\mu\nu} \propto \sqrt{-t'}^{\,|\mu-\nu-\mu'+\nu'|}$ as a consequence of angular momentum conservation.

This version of the amplitude $\mathcal{M}^{\rm pole}_{0-,++}$ is a generalization of the familiar result for photoproduction of pions. Electromagnetic gauge invariance provides a further argument for the version (10). Treating the pion and the nucleon as point-like particles (or with common form factors) and adding the contributions from nucleon exchange to the amplitudes (9)

$$\mathcal{M}^N \;=\; \frac{\sqrt{2}e_0 g_{\pi NN}}{W^2-m^2}\,\bar{u}(p',\nu')\gamma_5(\not{p}+\not{q}+m)\not{\epsilon}(\mu)u(p,\nu)\,, \tag{11}$$

(where W the c.m.s. energy of the process $\gamma^* p \to \pi^+ n$), one obtains a gauge invariant expression. At high energies however since $W^2-m^2 \simeq Q^2(1-\xi)/(2\xi)$, all the contributions from nucleon exchange are suppressed as compared to the amplitudes (9) with the exception of $\mathcal{M}^N_{0-,++}$ which has the form of the background term in (10). For a detailed discussion of gauge invariance and Reggeization see [23]. We are going to use (9) in our analysis with the amplitude $\mathcal{M}_{0-,++}$ modified according to (10).

It has been shown, for instance in Refs. [15, 24], that the pion pole contribution can be viewed as part of the GPD $\widetilde{E}$:

$$\widetilde{E}^u_{\rm pole} \;=\; -\widetilde{E}^d_{\rm pole} \;=\; \Theta(|\bar{x}|\le\xi)\,\frac{F_P(t)}{4\xi}\Phi_\pi((\bar{x}+\xi)/(2\xi))\,, \tag{12}$$

where F_P is the pseudoscalar form factor of the nucleon being related to $\widetilde{E}$ by the sum rule

$$\int_{-1}^{1} d\bar{x}\widetilde{E}^{(3)}(\bar{x},\xi,t) \;=\; F_P(t)\,. \tag{13}$$

With the help of PCAC and the Goldberger-Treiman relation the pseudoscalar form factor can be written as

$$F_P(t) \;=\; -mf_\pi\frac{2\sqrt{2}g_{\pi NN}F_{\pi NN}(t')}{t-m_\pi^2}\,. \tag{14}$$

Working out the convolution (3) for $\widetilde{E}^{(3)}_{\rm pole}$ one exactly obtains the pion pole contribution as given in (1) with, however, the perturbative result for the pion form factor obtained within the modified perturbative approach [25] or within its collinear approximation if one works with it. The perturbative result underestimates the experimental value of the form factor by about a factor of three for Q^2 in the range of $3-5$ GeV^2.

The measurement of the pion form factor bases on the fact that, at least at large ξ and small $-t$, the longitudinal cross section for π^+ electroproduction,

the process we are analyzing in this work, is dominated by the pion-pole contribution with some corrections from other sources (see below). For instance, the Jefferson Lab $F_\pi - 2$ collaboration [8] has recently measured the longitudinal cross section and analyzed these data with a Regge parameterization [26] leaving $F_\pi(Q^2)$ as a free parameter. The fit to their data provides

$$F_\pi(Q^2) \simeq \left[1 + Q^2/0.50 \ \text{GeV}^2\right]^{-1} . \tag{15}$$

Obviously, the use of the perturbative result only is in conflict with the very idea of measuring the pion form factor. We therefore refrain from using it in contrast to previous work, e.g. [15], and employ instead the experimental value (15) of the pion's electromagnetic form factor in the evaluation of the observables for π^+ electroproduction.

For the form factor of the pion-nucleon vertex we use the parameterization

$$F_{\pi NN}(t') \ = \ (\Lambda_N^2 - m_\pi^2)/(\Lambda_N^2 - t') \, , \tag{16}$$

where Λ_N is considered as an adjustable parameter.

Alternatively, one may use a reggeized version of pion exchange which is obtained from (9) by the replacement

$$\frac{1}{t - m_\pi^2} \Longrightarrow \frac{\pi\alpha'_\pi}{2} \left(\alpha_\pi(t) + 1\right) \frac{1 + \exp[-\imath\pi\alpha_\pi(t)]}{\sin \pi\alpha_\pi(t)} \left(\frac{W}{W_0}\right)^{2\alpha_\pi(t)} . \tag{17}$$

For the pion trajectory one may take the usual linear form

$$\alpha_\pi(t) \ = \ \alpha'_\pi(t - m_\pi^2) \, , \tag{18}$$

with the slope $\alpha'_\pi = 0.72 \ \text{GeV}^{-1}$ as is fixed by the masses and the spins of the π and the $\pi_2(1670)$ mesons. The value of the slope is somewhat smaller than the standard Regge slope of about $0.9 \ \text{GeV}^{-1}$ owing to Goldstone boson nature of the pion. Without this symmetry effect the pion mass would be roughly the same as the ρ mass leading to the standard slope. The scale W_0 may be chosen to be 1 GeV. The pion-nucleon form factor can be ignored in the reggeized version. Since, at large Q^2, only data at practically constant value of W are available [9] both variants of pion exchange lead to fits of more or less the same quality. The results presented below are obtained with the non-reggeized version.

W [GeV]	Q^2 [GeV^2]	$-t'$ [GeV^2]	$d\sigma_L/dt$	pole	$d\sigma_T/dt$	pole
2.308	2.215	0.000	2.078 ± 0.180	2.785	1.635 ± 0.11	0.359
2.264	2.279	0.037	1.365 ± 0.125	1.692	1.395 ± 0.08	0.243
2.223	2.411	0.050	0.980 ± 0.110	1.342	1.337 ± 0.08	0.216
2.181	2.539	0.060	0.786 ± 0.114	1.105	1.304 ± 0.08	0.200
2.127	2.703	0.087	0.564 ± 0.123	0.775	1.240 ± 0.08	0.164

Table 1: The longitudinal and transverse cross sections for π^+ electroproduction at low values of W in μb/ GeV^2. Quoted are the data of [8] and the contributions from the pion pole.

4 Transversely polarized photons

Here, in this section we want to argue that there is clear evidence for contributions from transversely polarized photons in the existing data on hard π^+ electroproduction.

An information on contributions from such photons comes from the recent Jefferson Lab measurement [8] of the separated cross sections at, however, the low energy of $\simeq 2.2$ GeV. The transverse cross section is sizeable; for $-t \gtrsim 0.2$ GeV^2 it is even larger than the longitudinal one. The importance of the pion pole is demonstrated in Tab. 1 where its contribution is confronted to the to the Jefferson Lab data [8]. The pion-pole contribution is evaluated from (9) and (10) with the help of (15) and (16) with $\Lambda_N = 0.51$ GeV. We use this value of Λ_N throughout this work. One observes that the longitudinal cross section is indeed dominated by the pole contribution, it even overshoots the data somewhat [4]. On the other hand, the pole contribution to the transverse cross section is much smaller than experiment. There is clear evidence for other contributions from transversely polarized photons.

An even more striking evidence for contributions from transversely polarized photons comes from the recent HERMES measurement of the asym-

[4] The dominance of the pion contribution to the longitudinal cross section has been also found in a recent Regge analysis of π^+ electroproduction [27].

metry, A_{UT}, for a transversely polarized target [10]. Various $\sin\Phi$-moments can be extracted from the measured differential cross section, where Φ is a linear combination of the azimuthal angle ϕ between the lepton and the hadron plane and the angle ϕ_S that describes the orientation of the target spin vector with respect to the lepton plane. The associated coefficients $A_{UT}^{\sin\Phi}$ are defined in the appendix; their relations to the helicity amplitudes are given in (44) (cf. also Tab. 2). The $\sin\phi_S$ moment is particularly large, only mildly t dependent and does not show any indication of a turnover towards zero for $t' \to 0$, see Fig. 2. Inspection of (44) reveals that this behavior of $A_{UT}^{\sin\phi_S}$ at small $-t'$, can only be produced by the longitudinal-transverse interference term $\mathrm{Im}\Big[\mathcal{M}^*_{0-,++}\mathcal{M}_{0+,0+}\Big]$. Both the contributing amplitudes are helicity non-flip ones and are therefore not forced to vanish in the forward direction by angular momentum conservation. The other interference term occurring for $A_{UT}^{\sin\phi_S}$ falls off proportional to t' for $t' \to 0$ by the same conversation law. The longitudinal amplitude $\mathcal{M}_{0+,0+}$ contributing to $A_{UT}^{\sin\phi_S}$ comprises the asymptotically dominant leading-twist contribution (1). The other amplitude in this interference term, $\mathcal{M}_{0-,++}$, which as we explained in the preceding section, plays a special role for the pion-pole contribution, remains to be discussed. It cannot solely be fed by the pole contribution (10) since, in this case, it would only interfere with the GPD contribution to $\mathcal{M}_{0+,0+}$ given in (1). As can readily be checked this contribution is too small (see Fig. 2). Hence, there must be another dynamical mechanism contributing to $\mathcal{M}_{0-,++}$.

It is tempting to model the amplitude $\mathcal{M}_{0-,++}$ from the ordinary GPDs $\widetilde{H}$, and so on. It is easy to check however that in this case the leading-twist pion spin wave function $q'\cdot\gamma\,\gamma_5/\sqrt{2}$ leads to $\mathcal{M}_{0-,++} = 0$. A more complicated spin wave function ivolving quark transverse momenta, would lead to a non-vanishing contribution but this one would vanish $\propto t'$ for $t' \to 0$. This behavior is a consequence of the fact the partons emitted and re-absorbed by the nucleon have the same helicity for these GPDs. Therefore, the hadronic matrix element for the transition $p(+)q(+) \to n(-)q(+)$ has to disappear as $\sqrt{-t'}$ as consequence of angular momentum conservation [17]. Moreover, the subprocess is described by the amplitude $\mathcal{H}_{0+,++}$ in this case which drops as $\sqrt{-t'}$, too. We conclude: In order to obtain a non-vanishing $A_{UT}^{\sin\phi_s}$ the amplitude $\mathcal{M}_{0-,++}$ has to be fed by dynamics that differs from that one taken into account by a handbag approach which includes only the helicity non-flip GPDs. This conclusion is conform with the observation that the pion-pole

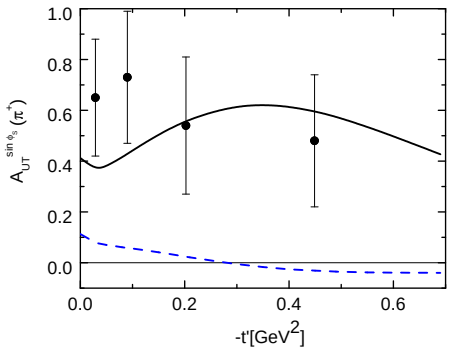

Figure 2: The $\sin\phi_s$ moment for a transversely polarized target at $Q^2 \simeq 2.45$ GeV^2 and $W = 3.99$ GeV. The prediction from our handbag approach is shown as a solid line. The dashed line is obtained disregarding the twist-3 contribution. Data are taken from [10]. (colors online)

contribution to the transverse cross section is clearly below experiment [8].

As a side remark we note that one observes in electroproduction of pions the same phenomenon as in photoproduction: The pion pole including the modification (10) is insufficient to describe the differential cross section at and near $t = 0$. Additional contributions to $\mathcal{M}_{0-,++}$ are required which, in the Regge approach, are typically modelled as Regge cuts [22, 28]. A similar observation can also be made in $p\bar{p} \to n\bar{n}$ [29]. The peculiar dynamics of photoproduction is qualitatively transferred to the transverse amplitudes of electroproduction in the Regge model. Quantitatively, however, modifications may occur since Regge residues and perhaps even the trajectories depend on Q^2 in general [30, 31].

5 A twist-3 contribution

There is a second set of four GPDs [17, 32] parameterizing the soft proton matrix elements. The partons emitted and absorbed by the nucleons have opposite helicities for these GPDs. Not much is known about them which are denoted by $H_T, \widetilde{H}_T, E_T$ and $\widetilde{E}_T$. There are only a few papers to be found in the literature in which they have been applied, e.g. in [35] to electroproduction of two vector mesons, in [33] to wide-angle photoproduction of pions or in [34] to π^0 electroproduction. In contrast to the ordinary GPDs which are

$\gamma^+(\gamma_5)$ proton matrix elements of quark field operators the helicity flip ones are σ^{+j} matrix elements where $j(=1,2)$ is a transverse index. As one can readily convince oneself by simply counting the number of gamma matrices in the relevant lowest-order Feynman graphs for the subprocess (see Fig. 1), the leading-twist pion spin wave function $q' \cdot \gamma \, \gamma_5/\sqrt{2}$ leads to a vanishing amplitude. Hence, one has to apply the pion's twist-3 spin wave functions.

The contributions of the twist-3 mechanism to the helicity amplitudes read

$$\begin{aligned}
\mathcal{M}^{\rm twist-3}_{0+,\mu+} &= e_0 \frac{\sqrt{-t'}}{2m} \int_{-1}^{1} d\bar{x} \, \Big\{ (\mathcal{H}_{0+,\mu-} - \mathcal{H}_{0-,\mu+}) \widetilde{H}_T^{(3)} \\
&+ [(1-\xi)\mathcal{H}_{0+,\mu-} - (1+\xi)\mathcal{H}_{0-,\mu+}] E_T^{(3)}/2 \\
&+ [(1-\xi)\mathcal{H}_{0+,\mu-} + (1+\xi)\mathcal{H}_{0-,\mu+}] \widetilde{E}_T^{(3)}/2 \Big\} \\
\mathcal{M}^{\rm twist-3}_{0-,\mu+} &= e_0 \sqrt{1-\xi^2} \int_{-1}^{1} d\bar{x} \, \left\{ (\mathcal{H}_{0+,\mu-} - \mathcal{H}_{0-,\mu+}) \frac{t'}{4m^2} \widetilde{H}_T^{(3)} \right. \\
&+ \left. \mathcal{H}_{0-,\mu+} [H_T^{(3)} - \frac{\xi}{1-\xi^2} (\xi E_T^{(3)} - \widetilde{E}_T^{(3)})] \right\} . \qquad (19)
\end{aligned}$$

The amplitudes are generalizations of the wide-angle results derived in [33]. Given that we are interested in rather small ξ and small $-t'$ the dominant twist-3 contribution comes from H_T and occurs in the amplitude $\mathcal{M}_{0-,++}$ which importance we have discussed in Sec. 4. The amplitude $\mathcal{M}_{0-,-+}$ although also fed by H_T is suppressed by the factor t'/Q^2 generated by the double helicity-flip subprocess amplitude $\mathcal{H}_{0-,-+}$. Also the twist-3 contributions to the longitudinal amplitudes can be neglected; they come together with the subprocess amplitude $\mathcal{H}_{0\mp,0\pm}$ and are therefore suppressed by $\sqrt{-t'}/Q$ as compared to the H_T contribution to $\mathcal{M}_{0-,++}$.

A complete twist-3 pion wave function would include a pseudoscalar and a tensor two-particle term and in addition a three-particle contribution [36]. Although it cannot be justified theoretically except for $Q^2 \to \infty$, the latter is usually neglected in applications [33, 37, 38]. We also do so in order to accomplish a first, admittedly rough estimate of the twist-3 contribution to π^+ electroproduction. In general, however, the three-particle contribution may play an important role in reliable estimates of higher-twist contributions as well as in achieving gauge invariant amplitudes in general higher-twist scenarios [39].

According to Beneke and Feldmann [37], the light-cone projection operator of an outgoing pion in momentum space, including the twist-2 and 3

two-particle contributions, reads

$$\mathcal{P}^{\pi(ab)}_{\alpha\beta,kl} \;=\; \frac{f_\pi}{2\sqrt{2N_c}}\,\mathcal{C}^{ab}_\pi\,\frac{\delta_{kl}}{\sqrt{N_c}}\left\{\frac{\gamma_5}{\sqrt{2}}\,\not{q}'\Phi_\pi(\tau)\;+\;\mu_\pi\,\frac{\gamma_5}{\sqrt{2}}\Big[\Phi_{\pi\,p}(\tau)\right.$$
$$\left.-i\sigma_{\mu\nu}\frac{q'^{\,\mu}k'^{\,\nu}}{q'\cdot k'}\frac{\Phi'_{\pi\,\sigma}(\tau)}{6}+i\sigma_{\mu\nu}q'^{\,\mu}\frac{\Phi_{\pi\,\sigma}(\tau)}{6}\frac{\partial}{\partial k_{\perp\nu}}\Big]\right\}_{\alpha\beta}\,, \qquad (20)$$

where α (a, k) and β (b, l) represent Dirac (flavor, color) labels of the quark and antiquark, respectively. This version of the projector which is the one proposed in [37] conveniently rewritten in the notation of [40], can be found in [33]. The parameter μ_π is not just the pion mass but it is proportional to the chiral condensate

$$\mu_\pi \;=\; m_\pi^2/(m_u+m_d)\,. \qquad (21)$$

The masses m_u and m_d in (21) are current quark masses [41]. At a scale of 2 GeV μ_π has the familiar value of $\simeq 2$ GeV. In (20), $\mathbf{k}_\perp$ denotes the transverse momentum of the quark entering the meson, defined with respect to the meson's momentum, q'. After performing the derivative the collinear limit, $\mathbf{k}_\perp = 0$, is taken. Note that in the massless limit we are working in, the two vectors q' and k' being the momentum of the outgoing parton, are light-like and their space components have opposite sign. The projector takes into account the familiar twist-2 distribution amplitude $\Phi_\pi(\tau)$ and the two-particle twist-3 ones $\Phi_{\pi\,p}(\tau)$ and $\Phi_{\pi\,\sigma}(\tau)$. In (20), $\Phi'_{\pi\,\sigma}$ denotes the derivative of $\Phi_{\pi\,\sigma}$ with respect to τ. The use of the twist-3 part of the projector within the modified perturbative approach is fully analogous to that of the twist-2 piece, see [5, 6].

Assuming the three-particle distributions to be strictly zero, the equation of motion fix the twist-3 distribution amplitudes [36, 37] to:

$$\Phi_{\pi\,p}(\tau) \;=\; 1\,, \qquad \Phi_{\pi\,\sigma}(\tau) \;=\; 6\,\tau\,(1-\tau)\,. \qquad (22)$$

The flavor weight factors $\mathcal{C}^{ab}_\pi$ comprise the flavor structure of the meson. They read

$$\mathcal{C}^{uu}_{\pi^0} = -\,\mathcal{C}^{dd}_{\pi^0} = 1/\sqrt{2}\,, \qquad \mathcal{C}^{ud}_{\pi^+} = \mathcal{C}^{du}_{\pi^-} = 1\,, \qquad (23)$$

for charged and uncharged pions. All other weight factors are zero (e.g., $\mathcal{C}^{ss}_{\pi_0} = 0$) since the projection operator (20) implies the valence quark approximation for the meson.

The twist-3 subprocess amplitude $\mathcal{H}_{0-,++}$ to lowest order of perturbative QCD is to be calculated from the same set of Feynman graphs as the twist-2

contribution (see Fig. 1). It turns out that the tensor terms provide contributions which are proportional to t'/Q^2 and are consequently neglected by us. Thus, only the pseudoscalar contribution to $\mathcal{H}_{0-,++}$ remains at small $-t$. As for the twist-2 contributions we calculate it within the modified perturbative approach and obtain ($\bar\tau = 1-\tau$)

$$\begin{aligned}\mathcal{H}^{\pi^+}_{0-,++} &= \frac{\sqrt{2}}{\pi}\frac{C_F}{\sqrt{N_c}}\mu_\pi \int d\tau d^2\mathbf{k}_\perp \Psi_{\pi\, p}(\tau,\mathbf{k}_\perp)\alpha_{\rm s}(\mu_R) \\ &\times \left(\frac{e_u}{\bar x-\xi+\imath\varepsilon}\,\frac{1}{\bar\tau(\bar x-\xi)Q^2/(2\xi)-\mathbf{k}_\perp^2+\imath\varepsilon}\right. \\ &+ \left.\frac{e_d}{\bar x+\xi-\imath\varepsilon}\,\frac{1}{\tau(\bar x+\xi)Q^2/(2\xi)+\mathbf{k}_\perp^2-\imath\varepsilon}\right). \qquad (24)\end{aligned}$$

In the spirit of the modified perturbative approach we only retain $\mathbf{k}_\perp$ in the denominators of the parton propagators where it plays a crucial role. Its square competes with terms $\propto \tau(\bar\tau)Q^2$ which become small in the end-point regions where either τ or $\bar\tau$ tends to zero. The expression (24) is to be Fourier transformed to the impact parameter space and there to be multiplied by the Sudakov factor $\exp[-S]$ analogously to (5). The LCWF corresponding to the pseudoscalar term is denoted by $\Psi_{\pi\, p}$. Evidently the twist-3 contribution is suppressed by μ_π/Q as compared to the twist-2 ones. The large value of μ_π provides the justification for making allowance for this twist-3 effect in our analysis while other contributions being parametrically suppressed by $\sqrt{-t'}/Q$, are omitted. We stress that, to the order of accuracy we are working, the amplitude (24) respects electromagnetic and color gauge invariance.

In collinear approximation $\mathcal{H}_{0-,++}$ is infrared singular since the corresponding distribution amplitude (22) does not vanish at the end points. Moreover, in collinear approximation there is a double pole $(\bar x-\xi)^2$. It is elucidating to compare with wide-angle photoproduction in collinear approximation [33, 42] where the Mandelstam variables t and u provide the large scale required by the handbag factorization. In collinear approximation the twist-3 contribution is regular in the wide-angle region, in fact zero by an exact cancellation of the pseudoscalar and the tensor terms, if the three-particle contribution is neglected [33]. The origin of this difference between deeply-virtual and wide-angle pion production lies in propagators of the type

$$B \propto \frac{t}{\tau t-\bar\tau Q^2}\,, \qquad (25)$$

occurring for the two tensor terms. Hence, in the wide-angle region one has

$$B \propto 1/\tau\,, \tag{26}$$

i.e. a contribution that has the same t dependence as the pseudoscalar term and an exact cancellation may happen and indeed takes place. On the other hand, for the case of electroproduction, one has

$$B \propto \frac{t}{\bar{\tau} Q^2}\,, \tag{27}$$

which cannot cancel the pseudoscalar term in the forward limit.

6 GPDs and meson wave functions

According to the discussion presented in Sec. 2 we need to model the GPDs $\widetilde{H}$ and $\widetilde{E}$ for valence quarks. For the twist-3 contribution we need the GPD H_T in addition. Throughout flavor-symmetric sea GPDs are assumed. We also have to discuss the pion LCWFs.

The GPDs $\widetilde{H}$, $\widetilde{E}$ and H_T for valence quarks are constructed from their double distribution representation. For the latter the familiar ansatz [43]

$$f_i^a(\rho,\eta,t) \;=\; \exp\left[(b_i - \alpha_i' \ln\rho) t\right] F_i^a(\rho, \xi = t = 0)\, \frac{3}{4} \frac{[(1-\rho)^2 - \eta^2]}{(1-\rho)^3}\, \Theta(\rho) \tag{28}$$

is made which consists of the forward limit, F_i, of the relevant GPD, a weight function and a t dependent factor parameterized in a Regge-like fashion with a Regge trajectory, $\alpha(t)$ and a residue function. The $t = 0$ part of this factor is absorbed into the forward limit of the GPD.

As in our previous work [7] the forward limit of $\widetilde{H}$, the polarized parton distributions, is taken from the analysis presented in [44]. The parameters in the t dependent factor are poorly determined as yet since the only sensitive experimental information in vector-meson electroproduction is provided by the helicity correlation A_{LL} for ρ^0 electroproduction measured by HERMES [45] and COMPASS [46]. These data suffer from very large errors. Since π^+ electroproduction offers a better handle on these parameters we fix them in the present analysis: $\tilde{\alpha}_h' \;=\; 0.45\ \mathrm{GeV}^{-2} t$ and $\tilde{b}_h = 0$.

Nothing is known about $\widetilde{E}$ as yet. In order to simplify matters we first assume that

$$\widetilde{E}^u \;=\; -\widetilde{E}^d \;=\; \frac{1}{2} \widetilde{E}^{(3)} \tag{29}$$

holds as for the perturbative part of the pion-pole term (12). This relation between the u and d quark GPDs is also similar to the situation for the GPD E [47, 48]. The forward limit of $\widetilde{E}^u$ is taken as

$$\tilde{e}^u(\rho) \;=\; \widetilde{N}_e \rho^{-0.48}(1-\rho)^5 \,. \tag{30}$$

For the t dependence we take the parameters $\widetilde{\alpha}'_e = 0.25\ \mathrm{GeV}^{-2}$ and $\tilde{b}_e = 0$. The value of the normalization $\tilde{N}_e$ is obtained from fits to the π^+ electroproduction data. We obtain $\tilde{N}_e = -25$.

The contribution from $\widetilde{E}$ has the opposite sign to the pion-pole contribution and becomes larger than the latter one for large $-t$. Our model GPD $\widetilde{E}^{(3)}$ is similar in size and sign to the results obtained in [24] where $\widetilde{E}$ has been calculated within the chiral soliton model. We have also checked that $\widetilde{E}$ and $\widetilde{H}$ respect the positivity bounds presented in [49, 50] (cf. the analogues of (193) and (194) in [50]).

In order to model the GPD H_T we rely on a model for the transversity distributions invented in Ref. [51] in order to fit the data on the azimuthal asymmetry in semi-inclusive deep inelastic scattering and in inclusive two-hadron production in electro-positron annihilation. The model proposed in [51] assumes that the transversity distributions which are the forward limit of the GPD H_T, are given by

$$\delta^q(\rho) \;=\; 7.46\, N_T^q\, \rho(1-\rho)^5 \left[q(\rho) + \Delta q(\rho)\right], \tag{31}$$

where q and Δq are the usual unpolarized and polarized parton distributions. In concord with [51] we take for the normalization constants the values

$$N_T^u \;=\; 0.5\,, \qquad N_T^d \;=\; -0.6\,. \tag{32}$$

For the slope of the Regge trajectory we again use $\alpha'_T = 0.45\ \mathrm{GeV}^{-2}$. The slope parameter b_T is adjusted to experiment leading to $b_T = 0.95\ \mathrm{GeV}^{-2}$. The resultant GPD is shown if Fig. 3 for sample values of the skewness.

For the pion LCWF we use a simple Gaussian [25]

$$\Psi_\pi \;=\; \frac{\sqrt{6}}{f_\pi} \exp\left[-a_\pi^2 \mathbf{k}_\perp^2/(\tau\bar{\tau})\right], \tag{33}$$

which has been probed in many applications. The transverse size parameter, a_π, is fixed from the $\pi^0 \to \gamma\gamma$ decay [52] to be

$$a_\pi \;=\; [\sqrt{8}\pi f_\pi]^{-1}\,. \tag{34}$$

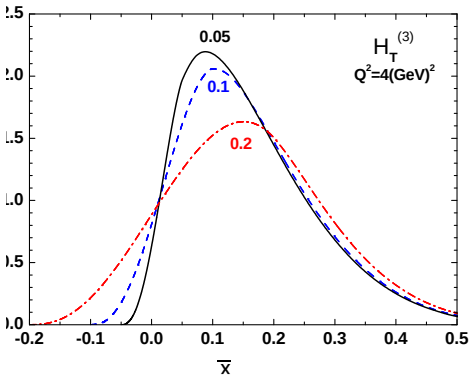

Figure 3: The isovector combination of the GPD H_T for versus $\bar{x}$ for $\xi = 0.05$ (solid), 0.1 (dashed) and 0.2 (dash-dotted line). (colors online)

The LCWF (33) corresponds to the twist-2 asymptotic meson distribution amplitude $\Phi_{AS} = 6\tau\bar{\tau}$. One may consider more general τ dependencies by multiplying Φ_{AS} with a sum of Gegenbauer terms [52]. Exploiting values of the lowest Gegenbauer coefficients derived from QCD sum rules [38, 53] or extracted from data on the $\pi\gamma$ transition form factor [54] lead to results for π^+ electroproduction which do not differ much from those obtained with Φ_{AS}. We therefore show only results for the latter case in the following.

For the pseudoscalar LCWF required for the calculation of the twist-3 contribution we take

$$\Psi_{\pi p} \;=\; \frac{16\pi^{3/2}}{\sqrt{6}}\, f_\pi a_\pi^3 k_\perp \exp\left[-a_p^2 \mathbf{k}_\perp^2\right], \tag{35}$$

which corresponds to the distribution amplitude $\Phi_{\pi p}$ quoted in (22). The combination of the two requirements, namely the constant distribution amplitudes and normalizibility of the wave function forces the use of the simple exponential which is to be contrasted with (33). The r.m.s. value of $\mathbf{k}_\perp$ is just $1/a_p$. In order to have $\langle \mathbf{k}_\perp^2 \rangle^{1/2} \simeq 0.5$ GeV a value of 2.0 GeV^{-1} is required for a_p [25].

observable	dominant interf. term	amplitudes	low t' behavior
$A_{UT}^{\sin(\phi-\phi_s)}$	LL	$\mathrm{Im}[\mathcal{M}^*_{0-,0+}\mathcal{M}_{0+,0+}]$	$\propto \sqrt{-t'}$
$A_{UT}^{\sin(\phi_s)}$	LT	$\mathrm{Im}[\mathcal{M}^*_{0-,++}\mathcal{M}_{0+,0+}]$	const.
$A_{UT}^{\sin(2\phi-\phi_s)}$	LT	$\mathrm{Im}[\mathcal{M}^*_{0-,-+}\mathcal{M}_{0+,0+}]$ [1)]	$\propto t'$
$A_{UT}^{\sin(\phi+\phi_s)}$	TT	$\mathrm{Im}[\mathcal{M}^*_{0-,++}\mathcal{M}_{0+,++}]$	$\propto \sqrt{-t'}$
$A_{UT}^{\sin(2\phi+\phi_s)}$	TT	$\propto \sin\theta_\gamma$	$\propto t'$
$A_{UT}^{\sin(3\phi-\phi_s)}$	TT	$\mathrm{Im}[\mathcal{M}^*_{0-,-+}\mathcal{M}_{0+,-+}]$	$\propto (-t')^{(3/2)}$
$A_{UL}^{\sin(\phi)}$	LT	$\mathrm{Im}[\mathcal{M}^*_{0-,++}\mathcal{M}_{0-,0+}]$	$\propto \sqrt{-t'}$

Table 2: Features of the asymmetries for a transversally and longitudinally polarized target. The photon polarization is denoted by L (longitudinal) and T (transversal). 1) There is a second contribution for which the helicities of the outgoing proton are interchanged.

7 Results from the handbag approach

In the preceding sections we have specified all the ingredients of our handbag approach to π^+ electroproduction and turn now to the calculation of observables and the comparison with experiment. The relations between observables and helicity amplitudes are compiled in the appendix.

It is to be stressed that the calculation of π^+ electroproduction is intriguing. Three, as yet practically unknown GPDs are needed. The t dependence of the data [8, 9, 10, 11] is much more complicated than that of diffractive vector-meson electroproduction [6, 7]. Is is also important to realize at this point that we model only one of the transverse amplitudes in detail, namely $\mathcal{M}_{0-,++}$. For the other transverse amplitudes we only consider the tiny pion-pole contribution. Moreover, the twist-3 effect can only be regarded as a rough estimated since the three-particle contribution to the pion state is ignored. For these reasons, we can only aim at an understanding of the gross feature of the data. A precise fit of all details of the data is beyond feasibility at present.

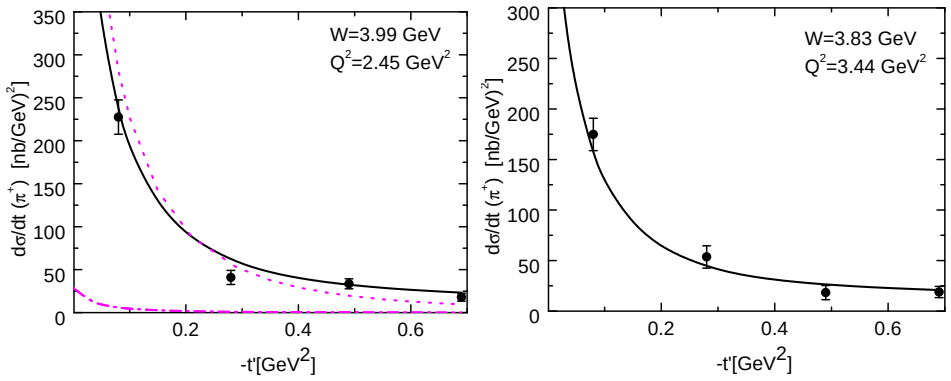

Figure 4: The un-separated π^+-electroproduction cross section versus $-t'$. The solid lines represent our predictions for the un-separated cross section. The dashed and dot-dashed lines are the pion-pole contributions for the un-separated and transversal cross sections, respectively. Data are taken from [9]. (colors online)

In Figs. 4 and 5 we show the un-separated differential cross section $d\sigma_T/dt + \epsilon d\sigma_L/dt$ at various values of Q^2 and W. We take $\epsilon = 0.8$ for the polarization of the virtual photon, a value that is characteristic of HERMES kinematics. As the comparison with the HERMES [9] data reveals we achieve a fair description of the cross section.

In Fig. 5 we also display the four partial cross sections. The longitudinal cross section is large and drops down rapidly with increasing $-t'$. Also the transverse cross section, essentially made up by the twist-3 mechanism is rather large. Hence, a considerable share of the un-separated cross section measured by HERMES [9] is due to contributions from transversely polarized photons. The longitudinal-transverse interference $d\sigma_{LT}/dt$ is particularly large at very small $-t'$ due to the interference between the pion-pole contribution to $\mathcal{M}_{0-,0+}$ and the twist-3 contribution to $\mathcal{M}_{0-,++}$. Since the first amplitude vanishes for forward scattering a pronounced bump is produced by the interference term $\mathrm{Re}[\mathcal{M}^*_{0-,++}\mathcal{M}_{0-,0+}]$. For large $-t'$ the LT cross section becomes negative. Not unexpectedly the TT cross section is very small.

Results for the asymmetries A_{UT} obtained with a transversely polarized proton target, are displayed in Figs. 2 and 6. In order to elucidate the behavior of the target asymmetries it is advisable to simplify the expressions (44)

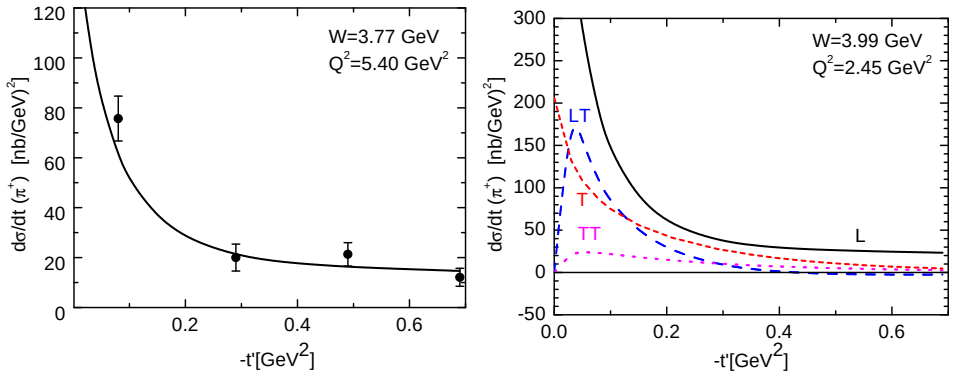

Figure 5: Left: As Fig. 4 but for $Q^2 = 5.4$ GeV^2 and $W = 3.77$ GeV. Right: The partial cross sections $d\sigma_L/dt$ (solid line), $d\sigma_T/dt$ (short dashed line), $d\sigma_{LT}/dt$ (long dashed line) and $d\sigma_{TT}/dt$ (dotted line) at $Q^2 = 2.45$ GeV^2 and $W = 3.99$ GeV. (colors online)

and (47) and to inspect the most prominent contributions. They and their behavior for $t' \to 0$ are listed in Tab. 2. The three moments $\sin(\phi + \phi_s)$, $\sin(2\phi + \phi_s)$ and $\sin(3\phi - \phi_s)$ are only fed by transverse-transverse interference terms and are therefore small in our approach. This result is in concord with the smallness of the TT cross section. The hierarchy of the moments at fixed Q^2 and W perceptible in Tab. 2 is in agreement with the findings of the HERMES collaboration [10]. Particularly large is the $\sin\phi_s$ moment, cf. Fig. 2. This is a consequence of the fact that it is determined by the interference of two large helicity non-flip amplitudes as we discussed in Sect. 4. The change of sign of the $\sin(\phi - \phi_s)$ moment at large $-t'$ (see Fig. 6) is due to the contribution from $\widetilde{E}$ which over-compensates the pole contribution to $\mathcal{M}_{0-,0+}$ there. In order to reproduce this feature of the A_{UT} data a large contribution from $\widetilde{E}$ is demanded. In absolute value the $\sin(\phi - \phi_s)$ moment is somewhat large in our approach as compared to experiment. In Fig. 6 we also show a result for this moment obtained by neglecting all contributions from transversely polarized photons. In this case the prediction is much too large in absolute value. The $\sin(2\phi - \phi_s)$ moment is small as is the experimental value. Only the change of the sign at large $-t'$ is not reproduced by us. This observable however is given by an interference terms between the longitudinal amplitudes and transversal one other than $\mathcal{M}_{0-,++}$. Thus, likely an improvement of this moment would require a detailed modeling of

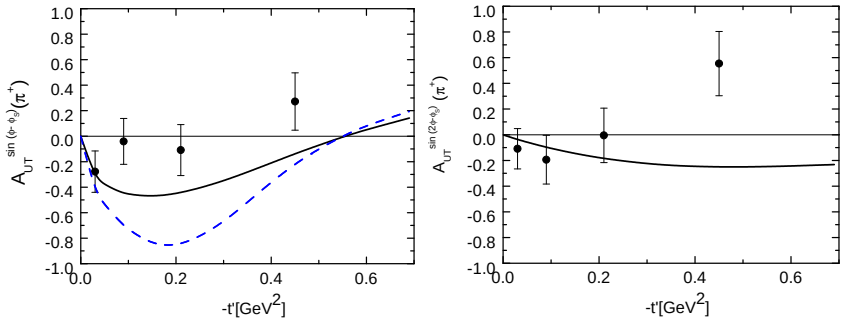

Figure 6: Predictions for the $\sin(\phi - \phi_s)$ (left) and the $\sin(2\phi - \phi_s)$ (right) moment at $Q^2 = 2.45$ GeV^2 and $W = 3.99$ GeV shown as solid lines. The dashed line represents the longitudinal contribution to the $\sin(\phi - \phi_s)$ moment. Data are taken from [10]. (colors online)

the small transverse amplitudes. In summary, it is fair to conclude that the pattern of the experimental results on the target asymmetries [10] is fully in agreement with the theoretical hierarchy. We finally mention that the Q^2 dependence of our predictions for the A_{UT} parameters at fixed t' and W is very smooth, typically the parameters decrease by about 10% in absolute value between $Q^2 = 2.5$ and 6 GeV^2.

The HERMES collaboration has also measured the asymmetry, A_{UL} for a longitudinally polarized target [11]. It is important to realize that A_{UL} is dominated by the interference term (see (47) and Tab. 2)

$$A_{UL} \propto \mathrm{Im}\Big[\mathcal{M}^*_{0-,++}\mathcal{M}_{0-,0+}\Big]\,. \tag{36}$$

The second term $\propto \mathcal{M}_{0+,0+}$ in (47) is zero since the combination $\mathcal{M}_{0+,++} + \mathcal{M}_{0+,-+}$ is zero in our approach, see (9). The interference term in (36) is similar to the one being responsible for the $\sin(\phi_s)$ moment obtained with a transversally polarized target. Only that instead of the longitudinal helicity non-flip amplitude, the helicty flip one occurs with the consequence of a small t' behavior as $\propto \sqrt{-t'}$ for A_{UL} making it smaller than $A_{UL}^{\sin(\phi_s)}$ in absolute value. In Fig. 7 we compare our results with the HERMES data on A_{UL} [11]. A good agreement between theory and experiment can be seen. In Figs. 2 and 7 we also display results which are obtained by disregarding the twist-3 contribution. The important role of the twist-3 contribution for the interpretation of the spin asymmetries is clearly seen.

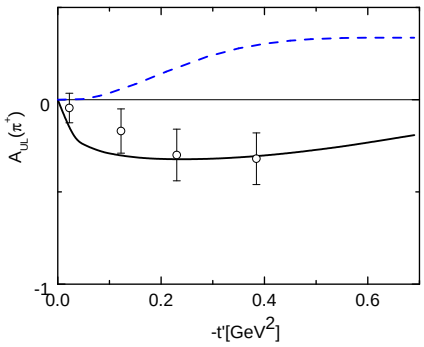

Figure 7: The asymmetry for a longitudinally polarized target at $Q^2 \simeq 2.4$ GeV^2 and $W \simeq 4.1$ GeV. The dashed line is obtained disregarding the twist-3 contribution. Data are taken from [11]. (colors online)

The asymmetry obtained with a longitudinally polarized beam is dominated by the interference term (36), too. But this asymmetry is smaller than A_{UL} by the factor $\sqrt{(1-\epsilon)/(1+\epsilon)} \simeq 1/3$.

Although the main purpose of this article is focussed on the analysis of the HERMES data one may be also interested in comparing our approach with the Jefferson Lab data on the cross sections [8]. However, a word of caution is advisable. It is known that the cross section for ρ^0 production shows an asymmetric minimum at $W \simeq 4$ GeV as a function of energy but at fixed Q^2. Between 2 and 4 GeV the cross section falls down by nearly an order of magnitude [55] while above 4 GeV it rises slowly, see [6] and references therein. On the other hand, the cross section for ϕ production increases for all energies above 2 GeV [6, 56, 57]. The handbag approach proposed by us [6, 7] is in perfect agreement with the slow increase of the cross sections for ρ^0 and ϕ production but the sharp rise below 4 GeV is not reproduced. What dynamical mechanism is responsible for that feature of the data is unknown as yet. One may surmise that the valence quarks are responsible for this peculiar behavior at low W since this effect is not seen in the cross section for ϕ production. Since π^+ production is solely fed by the valence quarks one may expect a similar failure of our handbag approach as for ρ^0 production. In order to examine whether or not this is the case we work out the longitudinal and transverse cross sections within our approach at the kinematics of the $F_\pi - 2$ experiment. We find reasonable agreement

for the transverse cross section with the Jefferson Lab data [8] while the longitudinal cross section is somewhat too small as compared to experiment. This failure is caused by the strong increase of the contribution from $\widetilde{E}$ with increasing skewness in comparison to the pion-pole contribution due to the extra factor of ξ in (1) which leads to a strong cancellation of these two terms. A strong $\widetilde{E}$ is required by the HERMES data on the spin asymmetries [10, 11]. Thus, we see that the application of our handbag approach at small W, i.e. large ξ, is problematic although not as drastic as for the case of the ρ^0. It however remains to be answered whether this difficulty is due to our particular model GPDs or whether one sees here other dynamics which cannot be incorporated into the handbag approach like in the case of the ρ^0. We stress that our approach is designed for small skewness. At larger values of it our parameterization of the GPDs (30) and (31) are perhaps to simple and may require improvements. Also the neglect of the helicity-flip GPDs E_T and $\widetilde{E}_T$ may not be justified at large skewness. Given all these uncertainties of our handbag approach we think that the results for low W are promising although a detailed investigation of this kinematical region is still necessary.

8 Electroproduction of π^0 mesons

Here, in this section, we are going to comment briefly on hard electroproduction of uncharged pions in the light of our findings for π^+ production. Now, instead of the isovector combination, we need $e_u F^u - e_d F^d$ where F is one of the GPDs $\widetilde{H}$, $\widetilde{E}$ or H_T. Since all the involved GPDs have opposite signs for u and d valence quarks there is a partial cancellation of the two contribution in contrast to π^+ production. Also the pion pole does not contribute in this case. Hence, a much smaller cross section is expected for π^0 production than for the case of π^+. On the other hand, a detailed experimental and theoretical study of π^0 electroproduction may provide distinct information on the relevant GPDs in the absence of the strong contributions from the pion pole.

The amplitudes now read (the flavor weight factors are defined in (23))

$$\begin{aligned}
\mathcal{M}^{\pi^0}_{0+,0+} &= \sqrt{1-\xi^2}\,\frac{e_0}{Q}\sum_{a=u,d} e_a\,\mathcal{C}^{aa}_{\pi^0}\Big[\,\langle\widetilde{H}^a\rangle - \frac{\xi^2}{1-\xi^2}\,\langle\widetilde{E}^a\rangle\Big]\,,\\
\mathcal{M}^{\pi^0}_{0-,0+} &= \frac{\sqrt{t_0-t}}{2m}\,\xi\frac{e_0}{Q}\sum_{a=u,d} e_a\,\mathcal{C}^{aa}_{\pi^0}\langle\widetilde{E}^a\rangle\,,
\end{aligned}$$

$$\mathcal{M}^{\pi^0}_{0-,++} \;=\; e_0\sqrt{1-\xi^2}\,\frac{\mu_\pi}{Q^2}\sum_{a=u,d} e_a\,\mathcal{C}^{aa}_{\pi^0}\,\langle H^a_T\rangle\,. \tag{37}$$

With the exception of the amplitudes which are related to those given in (37) by parity conservation, all other amplitudes are zero. Only valence quarks contribute electroproduction of uncharged pions.

The convolutions in (37) are given by expressions analogous to (3) with subprocess amplitudes like (5) or (24). The only difference is that the quark fractional charges e_a now appear in combination with the GPDs and not in the subprocess amplitudes (for more details cf. [48]). In the spirit of the modified perturbative approach we have to Fourier transform this expression and to multiply it with the Sudakov factor in the impact parameter space as in (5).

In Fig. 8 we present a few predictions for the un-separated cross section and the $A_{UT}^{\sin(\phi-\phi_s)}$ asymmetry for π^0 electroproduction. For typical HERMES kinematics the longitudinal cross section is dominant. We also see that the LT interference cross section is very small and exhibits a smooth t dependence. The pronounced peak at small $-t'$ seen for π^+ production (see Fig. 5) is absent. The $\sin(\phi-\phi_s)$ moment has the opposite sign as for π^+ production. The reason for these differences is the absence of the pion pole in π^0 electroproduction. For small energies, for instance at $W \simeq 2.2$ GeV, but the same value of Q^2 the cross section for π^0 production is more than a factor of 10 larger than at $W \simeq 4$ GeV. At this low energy the transverse cross section strongly dominates.

Our treatment of the twist-3 contribution differs from the approach proposed in [34] markedly. In the latter work the subprocess is viewed as form factors for photon-pion transitions under the action of vector and axial-vector currents. This is to be contrasted with our perturbative calculation which leads to a different helicity structure of the twist-3 contribution. Despite this strong contributions from transverse photons to electroproduction of pions are also found in [34] at $W \simeq 2.2$ GeV and $Q^2 \simeq 2.4$ GeV^2.

9 Twist-3 effects in vector-meson electroproduction

The twist-3 mechanism may also be applied to the amplitude $\mathcal{M}_{0-,++}$ for vector-meson production where the helicity label 0 now refers to a longitu-

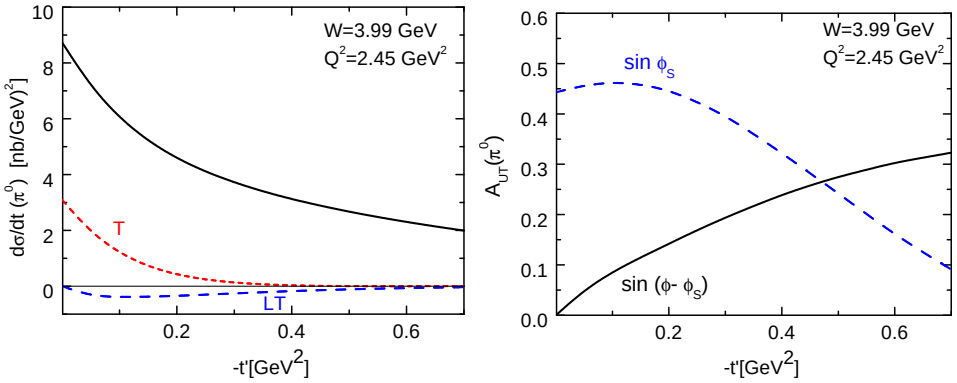

Figure 8: Predictions for the cross section (left) and A_{UT} (right) for π^0 electroproduction versus $-t'$ at $W = 3.99$ GeV and $Q^2 = 2.45$ GeV^2. The un-separated (transverse, longitudinal-transverse interference) cross section is shown as a solid (dashed, dotted) line. The $\sin(\phi - \phi_s)$ moment is shown as a solid line, the $\sin\phi_s$ moment as a dashed one. (colors online)

dinally polarized vector meson. This amplitude contributes to some of the spin density matrix elements (SDME), e.g. r^5_{00} in the notation of Schilling and Wolf [58], and influences also the transverse cross section. It is to be stressed that the parameter μ_π is now to be replaced by the vector-meson mass, m_V. The twist-3 effect is therefore parametrically of order m_V/Q which is not much larger than the generally neglected $\sqrt{-t'}/Q$ effects. The results presented in this section are therefore to be taken with a grain of salt, they are rather of qualitative nature.

The calculation of this twist-3 contribution to hard exclusive vector-meson electroproduction is fully analogous to the case of the pion. The subprocess amplitude is now to be calculated with the covariant spin wave function [5] $m_V/\sqrt{2}$ the analogue of the relevant twist-3 piece for pions (see (20)). It turns out that the subprocess amplitude $\mathcal{H}_{0-,++}$ is identically to (24) with the obvious replacements of μ_π by m_V and the pseudoscalar pion wave function by the corresponding vector-meson one, Ψ_{VP}. Thus, the twist-3 contribution

[5] We remind the reader that the polarization vector of a helicity-zero vector meson is $\epsilon(0) = q'/m_V$ up to corrections of order m_V/Q.

from the valence quarks to ρ^0 and ω production in momentum space reads

$$\mathcal{M}^V_{0-,++} \;=\; e_0\sqrt{1-\xi^2}\,\frac{m_V}{Q^2}\;\sum_{a=u,d} e_a\,\mathcal{C}^{aa}_V\;\langle H^a_T\rangle \tag{38}$$

in full analogy to (37). The flavor weight factors read

$$\mathcal{C}^{uu}_{\rho^0} \;=\; -\mathcal{C}^{dd}_{\rho^0} \;=\; \mathcal{C}^{uu}_{\omega} \;=\; \mathcal{C}^{dd}_{\omega} \;=\; 1/\sqrt{2} \tag{39}$$

for the vector mesons of interest in this work.

As we already mentioned the twist-3 effect in vector-meson electroproduction is smaller than in pion production since the large parameter μ_π is to be replaced by the vector-meson mass. Moreover, there is a partial cancellation between the u and d valence quark contributions since, according to (39), both partake in the combination $e_u H^u_T - e_d H^d_T$ as for the case of the π^0. Numerical evaluation indeed reveals that the twist-3 mechanism has no perceptible effect in ρ^0 electroproduction. For ω production the combination $e_u H^u_T + e_d H^d_T$ occurs which entails a larger twist-3 contribution than for the case of the ρ^0. Still the twist-3 effects is hardly noticeable. As an example we quote the ratio of the longitudinal and transverse cross sections for ω production. At $W = 5$ GeV and $Q^2 = 3$ GeV^2 the ratio amounts to 1.52 without and 1.4 with the twist-3 contribution. Thus, we can conclude that the results on vector-meson electroproduction presented in [6, 7] remain essentially unchanged by the inclusion of our twist-3 contribution. A detailed investigation of twist-3 and perhaps twist-4 contributions to vector-meson electroproduction is perhaps in order. Such an analysis which is beyond the scope of the present work, should also include the twist-3 mechanism for the gluonic subprocess and transversally polarized vector mesons.

10 Remarks on a symmetry property

It is well known that for natural (N) and unnatural (U) parity exchange the helicity amplitudes for meson electroproduction satisfy the relations

$$\begin{aligned}
\mathcal{M}^{MN}_{-\mu'\nu',-\mu\nu} &= \;\;\eta_M(-1)^{\mu-\mu'}\,\mathcal{M}^{MN}_{\mu'\nu',\mu\nu}\,,\\
\mathcal{M}^{MU}_{-\mu'\nu',-\mu\nu} &= -\eta_M(-1)^{\mu-\mu'}\,\mathcal{M}^{MU}_{\mu'\nu',\mu\nu}\,,
\end{aligned} \tag{40}$$

where, for vector mesons, η_M is +1 while for pseudoscalar mesons it is -1. In [5, 7] we have shown with the help of parity invariance

$$\mathcal{M}^{M}_{-\mu'-\nu',-\mu-\nu} \;=\; \eta_M(-1)^{\mu-\nu-\mu'+\nu'}\,\mathcal{M}^{M}_{\mu'\nu',\mu\nu}\,, \tag{41}$$

that at the twist-2 level (with or without power corrections like $\mathbf{k}_\perp$ effects) the handbag amplitudes have the property (40) too. The contributions from the GPDs H and E ($\widetilde{H}$ and $\widetilde{E}$) corresponds to (un)natural parity exchange. The absence of contributions from H and E in the longitudinal amplitudes for pion production (1) and (37) is also a consequence of (40). Obviously, the pion-pole amplitudes (9) corresponds to unnatural parity exchange. On the other hand, the modified pole amplitude $\mathcal{M}^{\rm pole}_{0-,++}$ (10) as well as the twist-3 contributions to $\mathcal{M}_{0-,++}$ given in (19), (37) and (38) do not possess the symmetry property (40). This readily follows from the fact that the subprocess amplitude $\mathcal{H}_{0-,-+}$ is double-flip one which vanishes at least $\propto t'$ for $t' \to 0$ in contrast to the non-flip amplitude $\mathcal{H}_{0-,++}$. Closer inspection of (19) reveals that not only contributions from H_T which we consider here in this work, do not possess the property (40) but also those from E_T and $\widetilde{E}_T$ while contributions from $\widetilde{H}_T$ behave like natural parity exchange.

11 Summary

Exclusive electroproduction of π^+ mesons at large Q^2 is investigated within the handbag approach. It is to be stressed that the process cannot be understood without taking into account pion exchange properly, i.e. the full experimentally measured electromagnetic form factor of the pion is to be employed; its asymptotically leading perturbative contribution is insufficient. In addition to the pion pole and the GPDs $\widetilde{H}$ and $\widetilde{E}$ a twist-3 contribution to the amplitude $\mathcal{M}_{0-,++}$ is required by the polarization data. In order to estimate the size of this effect which represents a correction of order μ_π/Q, we rely on a mechanism that consists of the helicity-flip GPD H_T and the twist-3 pion wave function. For the latter item only the two-particle partonic states are considered. This is perhaps a drastic approximation which admittedly allows only for a rather rough estimate of the size of the twist-3 contribution. All the subprocess amplitudes are calculated within the modified perturbative approach. Higher order perturbative corrections other than those included in the Sudakov factor (and in the experimental pion form factor) are not taken into account. According to Diehl and Kugler [59] the first order perturbative corrections are rather large for the cross sections for values of Q^2 around 3 GeV^2. However, we remind the reader that the corrections calculated by Diehl and Kugler refer to the leading-twist contribution only, i.e. to about 10% of the cross section. Finally we want to mention that our approach

applies to exclusive π^- electroproduction as well.

Acknowledgements We thank M. Diehl, I. Hristova and W.-D. Nowak for discussions. We are also grateful to the HERMES collaboration for providing us their data prior to publication. This work is supported in part by the Russian Foundation for Basic Research, Grant 09-02-01149 and by the Heisenberg-Landau program and by the BMBF, contract number 06RY258.

Appendix: Observables for $ep \to e\pi^+ n$

The unpolarized $ep \to e\pi^+ n$ cross section can be decomposed into a number of partial cross sections which are observables of the process $\gamma^* p \to \pi^+ n$

$$\begin{aligned}\frac{d^4\sigma}{dQ^2 dt d\phi} &= \frac{\alpha_{\rm elm}(s-m^2)}{16\pi^2 E_L^2 m^2 Q^2(1-\epsilon)}\left(\frac{d\sigma_T}{dt} + \epsilon\frac{d\sigma_L}{dt}\right. \\ &+ \left.\epsilon\cos 2\phi\,\frac{d\sigma_{TT}}{dt} + \sqrt{2\epsilon(1+\epsilon)}\cos\phi\frac{d\sigma_{LT}}{dt}\right). \qquad (42)\end{aligned}$$

The partial cross are expressed in terms of the $\gamma^* p \to \pi^+ n$ helicity amplitudes as follows

$$\begin{aligned}\frac{d\sigma_L}{dt} &= \frac{|\,\mathcal{M}_{0+,0+}\,|^2 + |\,\mathcal{M}_{0-,0+}\,|^2}{16\pi(W^2-m^2)\sqrt{\Lambda(W^2,-Q^2,m^2)}}, \\ \frac{d\sigma_T}{dt} &= \frac{|\,\mathcal{M}_{0-,++}\,|^2 + |\,\mathcal{M}_{0-,-+}\,|^2 + |\,\mathcal{M}_{0+,++}\,|^2 + |\,\mathcal{M}_{0+,-+}\,|^2}{32\pi(W^2-m^2)\sqrt{\Lambda(W^2,-Q^2,m^2)}}, \\ \frac{d\sigma_{LT}}{dt} &= -\frac{\sqrt{2}}{32\pi(W^2-m^2)\sqrt{\Lambda(W^2,-Q^2,m^2)}} \\ &\quad \mathrm{Re}\left[\mathcal{M}^*_{0-,0+}\Big(\mathcal{M}_{0-,++} - \mathcal{M}_{0-,-+}\Big) + \mathcal{M}^*_{0+,0+}\Big(\mathcal{M}_{0+,++} - \mathcal{M}_{0+,-+}\Big)\right], \\ \frac{d\sigma_{TT}}{dt} &= -\frac{\mathrm{Re}\Big[\mathcal{M}^*_{0-,++}\mathcal{M}_{0-,-+} + \mathcal{M}^*_{0+,++}\mathcal{M}_{0+,-+}\Big]}{32\pi(W^2-m^2)\sqrt{\Lambda(W^2,-Q^2,m^2)}}, \qquad (43)\end{aligned}$$

where L and T label longitudinally and transversally polarized virtual cross sections. The ep cross section for an unpolarized beam but a transversally

polarized target has been given by Diehl and Sapeta [60]. It consists of six terms which can be isolated by taking various sin-moments

$$
\begin{aligned}
A_{UT}^{\sin(\phi-\phi_s)}\sigma_0 &= -2\epsilon\cos\theta_\gamma\,\mathrm{Im}\Big[\mathcal{M}^*_{0-,0+}\mathcal{M}_{0+,0+}\Big] \\
&\quad -\cos\theta_\gamma\,\mathrm{Im}\Big[\mathcal{M}^*_{0+,++}\mathcal{M}_{0-,-+}-\mathcal{M}^*_{0-,++}\mathcal{M}_{0+,-+}\Big]\,, \\
&\quad +\frac{1}{2}\sin\theta_\gamma\sqrt{\epsilon(1+\epsilon)}\,\mathrm{Im}\Big[(\mathcal{M}^*_{0+,++}+\mathcal{M}^*_{0+,-+})\mathcal{M}_{0+,0+} \\
&\quad +(\mathcal{M}^*_{0-,++}+\mathcal{M}^*_{0-,-+})\mathcal{M}_{0-,0+}\Big] \\
A_{UT}^{\sin(\phi_s)}\sigma_0 &= \cos\theta_\gamma\sqrt{\epsilon(1+\epsilon)}\,\mathrm{Im}\Big[\mathcal{M}^*_{0+,++}\mathcal{M}_{0-,0+}-\mathcal{M}^*_{0-,++}\mathcal{M}_{0+,0+}\Big]\,, \\
A_{UT}^{\sin(2\phi-\phi_s)}\sigma_0 &= \cos\theta_\gamma\sqrt{\epsilon(1+\epsilon)}\,\mathrm{Im}\Big[(\mathcal{M}^*_{0+,-+}\mathcal{M}_{0-,0+}-\mathcal{M}^*_{0-,-+}\mathcal{M}_{0+,0+}\Big] \\
&\quad +\frac{1}{2}\epsilon\sin\theta_\gamma\,\mathrm{Im}\Big[\mathcal{M}^*_{0+,++}\mathcal{M}_{0+,-+}+\mathcal{M}^*_{0-,++}\mathcal{M}_{0-,-+}\Big]\,, \\
A_{UT}^{\sin(\phi+\phi_s)}\sigma_0 &= \epsilon\cos\theta_\gamma\,\mathrm{Im}\Big[\mathcal{M}^*_{0-,++}\mathcal{M}_{0+,++}\Big] \\
&\quad +\frac{1}{2}\sin\theta_\gamma\sqrt{\epsilon(1+\epsilon)}\,\mathrm{Im}\Big[(\mathcal{M}^*_{0+,++}+\mathcal{M}^*_{0+,-+})\mathcal{M}_{0+,0+} \\
&\quad +(\mathcal{M}^*_{0-,++}+\mathcal{M}^*_{0-,-+})\mathcal{M}_{0-,0+}\Big] \\
A_{UT}^{\sin(2\phi+\phi_s)}\sigma_0 &= \frac{1}{2}\epsilon\sin\theta_\gamma\,\mathrm{Im}\Big[\mathcal{M}^*_{0+,++}\mathcal{M}_{0+,-+}+\mathcal{M}^*_{0-,++}\mathcal{M}_{0-,-+}\Big]\,, \\
A_{UT}^{\sin(3\phi-\phi_s)}\sigma_0 &= \epsilon\cos\theta_\gamma\,\mathrm{Im}\Big[\mathcal{M}^*_{0+,-+}\mathcal{M}_{0-,-+}\Big]\,. \qquad (44)
\end{aligned}
$$

Here, ϕ is the azimuthal angle between the lepton and hadron plane and ϕ_s specifies the orientation of the target spin vector with respect to the lepton plane. The normalization σ_0 reads

$$
\begin{aligned}
\sigma_0 &= \frac{1}{2}\Big[\,|\,\mathcal{M}_{0+,++}\,|^2+|\,\mathcal{M}_{0-,-+}\,|^2+|\,\mathcal{M}_{0-,++}\,|^2+|\,\mathcal{M}_{0+,-+}\,|^2\,\Big] \\
&+ \epsilon\,\Big[\,|\,\mathcal{M}_{0+,0+}\,|^2+|\,\mathcal{M}_{0-,0+}\,|^2\,\Big]\,. \qquad (45)
\end{aligned}
$$

The angle θ_γ describes the rotation in the lepton plane from the direction of the incoming lepton to the the virtual photon one. It is given by [60]

$$
\cos\theta_\gamma = \sqrt{1-\gamma^2\,\frac{1-y-(y\gamma/2)^2}{1+\gamma^2}} \simeq 1-\frac{1}{2}\gamma^2(1-y)\,, \qquad (46)
$$

where $\gamma = 2x_{\mathrm{Bj}}m/Q$ and $y = (W^2+Q^2-m^2)/(s-m^2)$. Finally, ϵ is the ratio of the longitudinal and transversal photon fluxes.

Another observable of interest is the asymmetry for a longitudinally polarized target which is obtained from a $\sin\phi$-moment od the electroproduction cross section. In terms of the $\gamma^* p \to \pi^+ n$ helicity amplitudes it reads

$$\begin{aligned} A_{UL}\sigma_0 &= -\cos\theta_\gamma \sqrt{\epsilon(1+\epsilon)}\,\mathrm{Im}\Big[\Big(\mathcal{M}^*_{0+,++}+\mathcal{M}^*_{0+,-+}\Big)\mathcal{M}_{0+,0+} \\ &\quad +\Big(\mathcal{M}^*_{0-,++}+\mathcal{M}^*_{0-,-+}\Big)\mathcal{M}_{0-,0+}\Big] \\ &\quad +\sin\theta_\gamma\Big[2\epsilon\,\mathrm{Im}\Big(\mathcal{M}^*_{0-,0+}\mathcal{M}_{0+,0+}\Big)-\epsilon\,\mathrm{Im}\Big(\mathcal{M}^*_{0-,++}\mathcal{M}_{0+,++}\Big) \\ &\quad -\mathrm{Im}\Big(\mathcal{M}^*_{0-,++}\mathcal{M}_{0+,-+}-\mathcal{M}^*_{0+,++}\mathcal{M}_{0-,-+}\Big)\Big]\,. \end{aligned} \tag{47}$$

This leads to a contribution to the lepton-proton cross section as

$$d\sigma \sim P_L \sin\phi A_{UL} \tag{48}$$

where P_L is the target polarisation. The corresponding longitudinal beam polarization (P_l) reads

$$\begin{aligned} A_{LU}\sigma_0 &= -\cos\theta_\gamma \sqrt{\epsilon(1-\epsilon)}\,\mathrm{Im}\Big[\Big(\mathcal{M}^*_{0+,++}-\mathcal{M}^*_{0+,-+}\Big)\mathcal{M}_{0+,0+} \\ &\quad +\Big(\mathcal{M}^*_{0-,++}-\mathcal{M}^*_{0-,-+}\Big)\mathcal{M}_{0-,0+}\Big]\,. \end{aligned} \tag{49}$$

It contributes to the lepton-proton cross section as

$$d\sigma \sim P_l \sin\phi A_{LU}\,. \tag{50}$$

References

[1] D. Mueller *et al.*, Fortsch. Phys. **42**, 101 (1994) [hep-ph/9812448].

[2] A. V. Radyushkin, Phys. Lett. B **449**, 81 (1999) [hep-ph/9810466].

[3] K. Kumeričky and D. Müller, arXiv:0904.0458 [hep-ph].

[4] M. V. Polyakov and M. Vanderhaeghen, arXiv:0803.1271 [hep-ph].

[5] S. V. Goloskokov and P. Kroll, Eur. Phys. J. C **42**, 281 (2005) [hep-ph/0501242].

[6] S. V. Goloskokov and P. Kroll, Eur. Phys. J. C **50**, 829 (2007) [hep-ph/0611290].

[7] S. V. Goloskokov and P. Kroll, Eur. Phys. J. C **53**, 367 (2008) [arXiv:0708.3569 [hep-ph]].

[8] H. P. Blok *et al.* [Jefferson Lab Collaboration], Phys. Rev. C **78**, 045202 (2008) [arXiv:0809.3161 [nucl-ex]].

[9] A. Airapetian *et al.* [HERMES Collaboration], Phys. Lett. B **659**, 486 (2008) [arXiv:0707.0222 [hep-ex]].

[10] A. Airapetian *et al.* [HERMES Collaboration], arXiv:0907.2596 [hep-ex].

[11] A. Airapetian *et al* [HERMES Collaboration], Phys. Lett. B**535**, 85 (2002).

[12] L. Mankiewicz, G. Piller and T. Weigl, Eur. Phys. J. C**5**, 119 (1998).

[13] L. Mankiewicz, G. Piller and A.V. Radyushkin, Eur. Phys. J. C**10**, 307 (1999).

[14] L. L. Frankfurt, P. V. Pobylitsa, M. V. Polyakov and M. Strikman, Phys. Rev. D **60**, 014010 (1999) [arXiv:hep-ph/9901429].

[15] M. Vanderhaeghen, P. A. M. Guichon and M. Guidal, Phys. Rev. D **60**, 094017 (1999) [arXiv:hep-ph/9905372].

[16] J. Botts and G. Sterman, Nucl. Phys. B **325**, 62 (1989).

[17] M. Diehl, Eur. Phys. J. C**19**, 485 (2001) [hep-ph/0101335].

[18] J.C. Collins, L. Frankfurt and M. Strikman, Phys. Rev. D **56**, 2982 (1997) [hep-ph/9611433].

[19] A. Boyarski *et al*, Phys. Rev. Lett. **20**, 300 (1968).

[20] R. J. N. Phillips, Nucl. Phys. B**2**, 657 (1967).

[21] P. K. Williams, Phys. Rev. D **1**, 1312 (1970).

[22] M. Rahnama and J.K. Storrow, J. Phys. G **8**, 453 (1982).

[23] E. Leader, Acta Physica Austriaca, Suppl. VIII, 21 (1971).

[24] M. Penttinen, M. V. Polyakov and K. Goeke, Phys. Rev. D **62**, 014024 (2000) [arXiv:hep-ph/9909489].

[25] R. Jakob and P. Kroll, Phys. Lett. B **315**, 463 (1993) [Erratum-ibid. B **319**, 545 (1993)] [arXiv:hep-ph/9306259].

[26] M. Vanderhaeghen, M. Guidal and J. M. Laget, Phys. Rev. C **57**, 1454 (1998).

[27] M. M. Kaskulov and U. Mosel, arXiv:0904.4442 [hep-ph].

[28] R. Worden, Nucl. Phys. B**37**, 253 (1972).

[29] E. Leader, Phys. Lett. B**60**, 290 (1976).

[30] P. D. B. Collins and T. D. B. Wilkie, Z. Phys. C**7**, 357 (1981).

[31] A. Donnachie and P. V. Landshoff, arXiv:0803.0686 [hep-ph].

[32] P. Hoodbhoy and X. Ji, Phys. Rev. D**58**, 054006 (1998) [hep-ph/9801369].

[33] H. W. Huang, R. Jakob, P. Kroll and K. Passek-Kumericky, Eur. Phys. J. C**33**, 91 (2004) [arXiv:hep-ph/0309071].

[34] S. Ahmad, G. R. Goldstein and S. Liuti, Phys. Rev. D **79**, 054014 (2009) [arXiv:0805.3568 [hep-ph]].

[35] D. Y. Ivanov, B. Pire, L. Szymanowski and O. V. Teryaev, Phys. Lett. B **550**, 65 (2002) and Phys. Part. Nucl. **35**, S67 (2004). R. Enberg, B. Pire and L. Szymanowski, Eur. Phys. J. C **47**, 87 (2006).

[36] V. M. Braun and I. E. Filyanov, Z. Phys. **C48**, 239 (1990) [Sov. J. Nucl. Phys. **52**, 126 (1990) Yad. Fiz. **52**, 199 (1990)].

[37] M. Beneke and T. Feldmann, Nucl. Phys. B**592**, 3 (2001) [hep-ph/0008255].

[38] P. Ball, JHEP **9901**, 010 (1999) [hep-ph/9812375].

[39] I. V. Anikin, D. Y. Ivanov, B. Pire, L. Szymanowski and S. Wallon, arXiv:0903.4797, arXiv:0904.1482 [hep-ph].

[40] P. Kroll and K. Passek-Kumericki, Phys. Rev. D **67**, 054017 (2003) [hep-ph/0210045].

[41] C. Amsler *et al.* [Particle Data Group], Phys. Lett. B **667**, 1 (2008).

[42] H. W. Huang and P. Kroll, Eur. Phys. J. C**17**, 423 (2000) [arXiv:hep-ph/0005318].

[43] I. V. Musatov and A. V. Radyushkin, Phys. Rev. D **61**, 074027 (2000) [hep-ph/9905376].

[44] J. Blümlein and H. Böttcher, Nucl. Phys. B **636**, 225 (2002) [hep-ph/0203155]

[45] A. Airapetian *et al.* [HERMES Collaboration], Eur. Phys. J. C **29**, 171 (2003) [hep-ex/0302012].

[46] V. Y. Alexakhin *et al.* [COMPASS Collaboration], Eur. Phys. J. C **52**, 255 (2007) [arXiv:0704.1863 [hep-ex]].

[47] M. Diehl, T. Feldmann, R. Jakob and P. Kroll, Eur. Phys. J. C **39**, 1 (2005) [hep-ph/0408173].

[48] S. V. Goloskokov and P. Kroll, Eur. Phys. J. C **59**, 809 (2009) [arXiv:0809.4126 [hep-ph]].

[49] P. Pobylitsa, Phys. Rev. D **65**, 114015 (2002) [hep-ph/0201030].

[50] M. Diehl, Phys. Rept. **388**, 41 (2003) [hep-ph/0307382].

[51] M. Anselmino, M. Boglione, U. D'Alesio, A. Kotzinian, F. Murgia, A. Prokudin and C. Turk, Phys. Rev. D **75**, 054032 (2007) [arXiv:hep-ph/0701006].

[52] S. J. Brodsky, T. Huang and G. P. Lepage, *Banff 1981, Proceedings, Particle and Fields 2, 143-199.*

[53] A. P. Bakulev, S. V. Mikhailov and N. G. Stefanis, Phys. Lett. B **508**, 279 (2001) [Erratum-ibid. B **590**, 309 (2004)] [arXiv:hep-ph/0103119].

[54] M. Diehl, P. Kroll and C. Vogt
Eur. Phys. J. C **22**, 439 (2001) [arXiv:hep-ph/0108220].

[55] S. A. Morrow *et al* [CLAS collaboration], Eur. Phys. J. A**39**, 5 (2009) [arXiv:0807.3834 [hep-ex]].

[56] J. P. Santoro *et al.* [CLAS Collaboration], Phys. Rev. C **78**, 025210 (2008) [arXiv:0803.3537 [nucl-ex]].

[57] A. Borissov *et al* [HERMES Collaboration], proceedings of DIFFRACTION2000, Cosenza, Italy, September 2000; DESY-HERMES-00-055.

[58] K. Schilling and G. Wolf, Nucl. Phys. B **61**, 381 (1973).

[59] M. Diehl and W. Kugler, Eur. Phys. J. C **52**, 933 (2007) [arXiv:0708.1121 [hep-ph]].

[60] M. Diehl and S. Sapeta, Eur. Phys. J. C **41**, 515 (2005) [arXiv:hep-ph/0503023].